

# CFD Analysis of the Blood Flow in Left Coronary Bifurcation with Variable Angulation

Midiya Khademi, Ali Nikoo, Shabnam Rahimnezhad Baghche Jooghi

**Abstract**—Cardiovascular diseases (CVDs) are the main cause of death globally. Most CVDs can be prevented by avoiding habitual risk factors. Separate from the habitual risk factors, there are some inherent factors in each individual that can increase the risk potential of CVDs. Vessel shapes and geometry are influential factors, having great impact on the blood flow and the hemodynamic behavior of the vessels. In the present study, the influence of bifurcation angle on blood flow characteristics is studied. In order to approach this topic, by simplifying the details of the bifurcation, three models with angles 30°, 45°, and 60° were created, then by using CFD analysis, the response of these models for stable flow and pulsatile flow was studied. In the conducted simulation in order to eliminate the influence of other geometrical factors, only the angle of the bifurcation was changed and other parameters remained constant during the research. Simulations are conducted under dynamic and stable condition. In the stable flow simulation, a steady velocity of 0.17 m/s at the inlet plug was maintained and in dynamic simulations, a typical LAD flow waveform is implemented. The results show that the bifurcation angle has an influence on the maximum speed of the flow. In the stable flow condition, increasing the angle lead to decrease the maximum flow velocity. In the dynamic flow simulations, increasing the bifurcation angle lead to an increase in the maximum velocity. Since blood flow has pulsatile characteristics, using a uniform velocity during the simulations can lead to a discrepancy between the actual results and the calculated results.

**Keywords**—Coronary artery, cardiovascular disease, bifurcation, atherosclerosis, CFD, artery wall shear stress.

## I. INTRODUCTION

THE heart is a strong muscular organ about the size of the fist, pumping the blood in order to carry oxygen and nutrients to the whole body with each beat [1]. Good supply of food not only is essential for organs of the body but also it is vital for the normal function of the heart [2]. Providing the needs of heart for blood as shown in Fig. 1 (part A), there are many vessels (arteries and veins) placed on the heart. CVDs are a group of disorders that can affect heart and blood vessels and coronaries. According to WHO, CVDs are the main cause of death all around the world, and it is estimated that 17.5 million people lost their life because of CVDs in 2012 [3]. Heart attacks and strokes are usually acute events and mainly caused by a blockage that prevent blood from flowing through vessels into heart properly. The main reason of this disorder (atherosclerosis) is the build-up of fatty deposits (plaque) on

the inner walls of the arteries [4], which as shown in Fig. 1 (part B) narrow them and leads to reduce the blood flow to the heart [5]. Although habitual factors like using tobacco, physical activity, unhealthy diet, harmful use of alcohol, metabolic risk factors like hypertension, diabetes, and obesity can all increase the risk of developing atherosclerosis and coronary artery disease. There are some inherent factors like gender, genetic disorders [6], shape and geometries of the arteries that play roles in this process.

In certain flow conditions such as low shear stress (LSS) [7], flow disturbances are found to be related to atherogenic, then coronary geometries generating or exacerbating these phenomena, are in turn atherogenic [8]. The term "geometric risk factors" are used in order to demonstrate geometric features generating or enhancing a pre-existing atherogenic condition [9]. The curvatures and torsions are defined as "global geometric features" and cross-sectional shapes as "local geometric features," of the coronary arteries [10].

The blood flow characteristics determine the wall shear stress (WSS) and wall tension. The WSS and wall tension are closely related to the CVDs [11]. As a result, it is very important to predict the blood flow characteristics accurately in an efficient way for the CVD research, medical device design and surgical planning [12]. Even two-dimensional studies showed that WSS, stable pressure and near wall velocity magnitude exhibit the negative correlation to wall thickening. However, molecular viscosity exhibits the positive correlation to wall thickening [9]. Parameters such as the vessel compliance [10], [13], curvature [14], pulsatile blood flow [13], [14], and cardiac motion and myocardial contraction [14], [15] play roles on arterial wall stress/strain (WS/S) and vessel stiffness distribution [6].

As blood flow characteristics are closely related to various cardiovascular disease, so it is important to predict them accurate enough in the efficient way [12]. For fluid to a solid interaction between the wall of the artery and the blood [16], pressure condition is particularly important, but measuring pressure in vivo is highly invasive and difficult at the moment [17]. In order to investigate the human coronary arteries, two approaches of mathematical modeling and computer simulations are being used. Nowadays computer simulation not only promotes the arteries disorders calculation like atherosclerosis and aneurysm [18], but also it has great beneficent in understanding the mechanical behavior of coronary. While using this method, device manufacturers use a variety of experimental tests to ensure accurate properties like the stent, and artificial vascular, FEM methods can be used in order to forecast the influence of using stent [19]-[24],

Ali Nikoo is with the Department of Biomedical Engineering, Amirkabir University of Technology, Tehran, Iran.

Rahimnezhad Baghche Jooghi is with the School of Automotive Engineering, Iran University of Science and Technology, Tehran, Iran.

Midiya Khademi is PhD student of Biomedical Engineering, Young Researchers and Elites club, Science and Research Branch, Islamic Azad University, Tehran, Iran (e-mail: Midiya.khademi@srbiau.ac.ir).

or other endovascular aortic aneurysm repair [25].

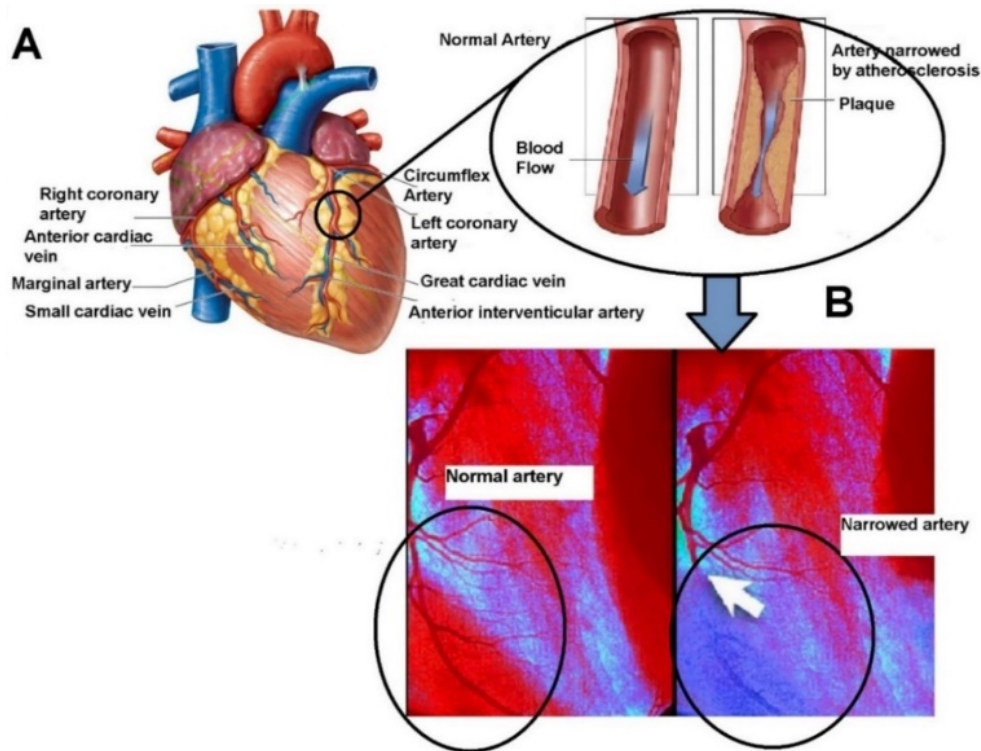


Fig. 1 A- Circumflex Coronary, B- Comparison between normal and narrowed artery

Smith et al. [26] investigate about magnitude of the WSS in coronary arteries and found that magnitude of the WSS was always greater in the interior of the LM (ranging from 0.75 Pa to 7.0 Pa during the cardiac cycle), than the interior of the LAD or LCX (ranging from 0.47 Pa to 3.2 Pa in the LAD and 0.20 Pa to 1.4 Pa in the LCX during the cardiac cycle). This could suggest that LAD and LCX are more delicate than the LM to the development of the atherosclerotic lesions that lead to cause coronary artery disease. It is generally accepted that atherosclerotic lesions develop in regions within the coronary artery where the WSS is low and oscillating. Since the LM, LAD, and LCX have roughly the same diameters, the greater WSS in the LM also suggests the axial fluid velocities in the LM are greater than those in the LAD and LCX. Therefore, it is reasonable to assume that flow velocities play an important role commencement of atherosclerosis and the further study of the velocity field in the coronary arteries is required [26].

Hemodynamics aspect of the artery is studied in some cases by neglecting the interaction between blood flow and arterial walls, evaluating the WSS at the rigid walls (Computer Fluid Dynamics, CFD Analysis), and other prefer to analyze the interaction between blood and the artery's wall, by using fluid-solid interaction analysis (FSI) [27]. Malve et al. showed the correlation between the WSS and the velocity field at the arterial wall which is similar for both CFD and FSI computations. Although they showed the discrepancy between their FSI and CFD simulation in amounts of WSS, the comparison between both results showed that the

consequences are completely in the same order and the maximum and minimum WSS in both simulations showed same behavior with shape of the artery. They mentioned that near the bifurcation the WSS is increased because of the separation of the blood flow in this area [9].

Tada et al. use FSI method in investigating bifurcation of the common carotid arteries. By calculating the WSS and circumferential stress-strain (CS) for the first time they defined stress phase angle (SPA) parameter, which is defined as a complex ratio of CS to WSS and they show that large negative SPA correlating with sites of plaque location[20]. Between the coronary arteries, bifurcations represent regions of the arterial tree that are susceptible to atherosclerotic lesions. Statistical data illustrate the angulation of the bifurcation might have an effect on shear stress and consequently on plaque size [28]. Coronary arterial bifurcations are prone to atherosclerosis development, and 20–30% of all percutaneous coronary interventions (PCI) involve bifurcations [5].

Rodriguez-Granillo studied on 50 patients that showed that more than 90% of plaques were located opposite to the flow divider, and normal ostial LAD bifurcation in the majority of the cases had a bifurcation angle  $< 88.5^\circ$  [29]. Sun and Cao studied on 30 patients' multislice CT angiography illustrates that the mean bifurcation angle between all of their case studies was measured about  $89.1^\circ \pm 13.1^\circ$  this value was about  $75.5^\circ \pm 19.8^\circ$  in normal case studies and it is about  $94^\circ \pm 19.7^\circ$  in disease case studies. According to their results, they believe

that there is a direct correlation between left bifurcation angle and dimensional changes and formation of plaque [23].

Important places for the formation of atherosclerosis are the outer wall of arterial bifurcations and the inside of curves where low WSS occurs or the shear stress changes direction during the cardiac cycle [14]. Malve et al. studied the unsteady flow and mass transfer of human left coronary artery bifurcation by using FSI and CFD method. Since they want to evaluate the maximum and the minimum WSS as a function of the flow regime and the arterial wall compliance in the left coronary, they use commercial finite element software. Their CFD and FSI analysis showed that WSS distributions were substantially affected by the arterial wall compliance [9]. It is also hypothesizing that the angulation of the bifurcation might have an effect on shear stress and consequently on plaque size. A wider bifurcation angle might be related to higher turbulence, whereas a narrow angle might be more prone to present laminar flow [28]. To the end of investigating the hemodynamic effect of variations in the angulations, Chaichana and his colleagues generated 12 models consisting of four realistic and eight simulated coronary artery geometries. The simulated models included various coronary artery angulations, namely, 15°, 30°, 45°, 60°, 75°, 90°, 105°, 120°. They find that there is a direct correlation between coronary angulations and subsequent hemodynamic changes, based on realistic and simulated models [30]. Beier and his colleagues study the impact of bifurcation angle on blood flow of non-stented and stented coronary arteries. In their studies, bifurcations with angles 40°, 60°, and 80° have been studied. In contrast with the previous studies, their study shows that bifurcation angle had minor impact on the areas of adverse hemodynamics in the idealized non-stented geometries, but stenting leads to a great change in the WSS value of bifurcation [24]. In the similar result, Chiastra et al. in their studies on different bifurcation angles and cardiac curvatures

for both stenosed and unstenosed bifurcations show that bifurcation angle impacts lowly hemodynamics in both stenosed and unstenosed cases. Instead, curvature radius influences the generation and transport of helical flow structures, with smaller cardiac curvature radius associated to higher helicity intensity [5].

In comparison with the right artery, the left artery has a very short main stem, which quickly divides into left anterior descending and left circumflex with an angle formed between these two branches [23]. The variation in the angulation supposed to be one of the influential parameters in blood flow characteristics. The main parameter that has great influence on the WSS is velocity distribution. In this study, the hemodynamic of blood is investigated by using simplified bifurcation model, and variable angulations [31]. In the first step of the simulation, the stable condition is considered and the input and output velocity and pressure do not change during the time step of the calculation, then in the second part, the dynamic condition imposed on the simulation by introducing pulsatile velocity.

## II. METHOD

### A. Artery Modeling and Numerical Grid Generation

Chaichana et al. consider realistic angle in their studies and investigate bifurcations ranges from 15° to 120° [30]. In this study three left coronary bifurcations in three angles included 30°, 45°, 60° is constructed. As shown in Fig. 2 (B), three-dimensional (3D) simplified models are created in commercial software (CATIA V5) according to the available data from. The arterial bifurcation in this study included left main coronary artery (LM) and its principal branches: the left anterior descending (LAD) and the left circumflex artery (LCX).

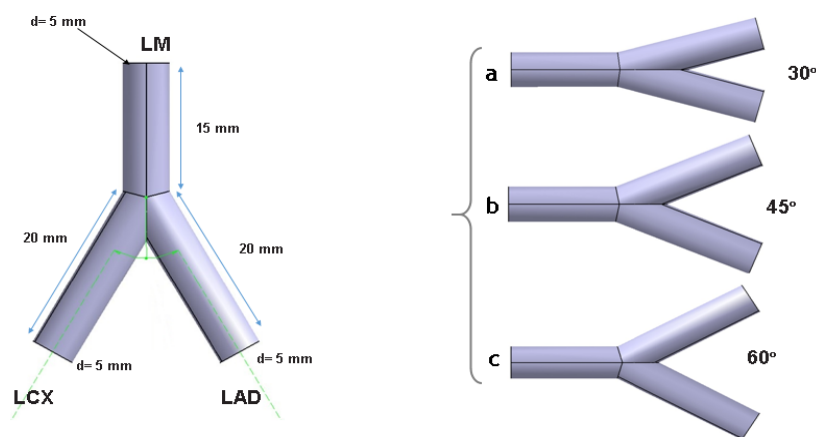


Fig. 2 A- Main dimension of the bifurcation, B- Bifurcation with variable angulation

Then the 'STL formats' are imported to commercial software for creating the meshes, and CFD analysis. To the end of CFD analysis, the wall is considered as rigid [32]. The fluid tetrahedral meshes are generated and as usual, in order to

establish the adequate element size for the computations, a sensitivity analysis was conducted on the bifurcation model with 30° in dynamic simulations. According to Table I, six different grids are generated to evaluate the acceptable results.

TABLE I  
SENSIVITY ANALYSIS

	Number of elements	The average size of elements	Maximum velocity (m/s)
1	1231	0.0025	0.07253
2	1419	0.0020	0.07260
3	4086	0.0014	0.07261
4	11589	0.0009	0.07256
5	103962	0.0004	0.07257
6	2869709	0.0001	0.07255

In each simulation, all the material and geometries

properties of the model remained constant and just the number of the meshes are changed and the value of the maximum velocity is recorded and compared with the previous results. As shown in Fig. 3, this procedure continued until when the difference between the result of the current simulation and the previous simulation reached to less than 0.02 percent. According to the results of the analysis, mesh cardinality for the 60° model is ~ 2870000 and approximate global size of the seeds equal to 0.0009 mm is chosen for the total simulations (Fig. 3 (B)).

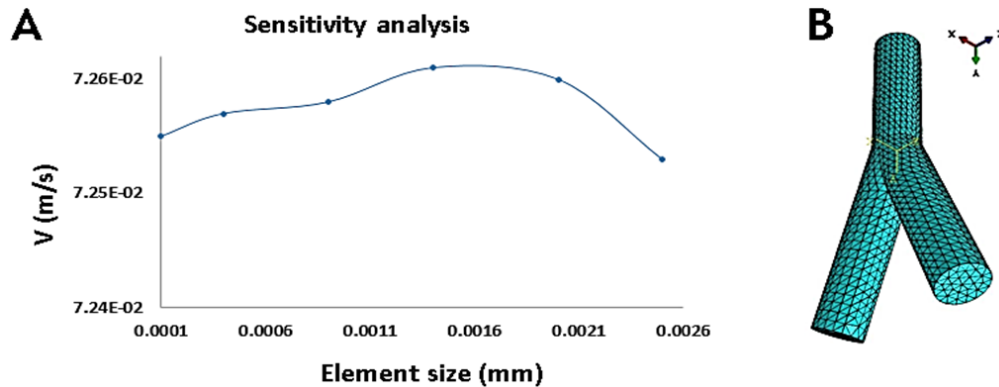


Fig. 3 A-Sensitivity analysis, B- Final mesh on 60° bifurcation

#### B. Materials of the Blood

Blood viscosity (non-Newtonian fluid) depends on shear rate, which is determined by blood platelets, red cells, etc. As reported in [10], the blood rheology is assumed as Newtonian; also, the blood density and the blood viscosity are considered as 1050 kg/m<sup>3</sup>, and 0.003528 Pa respectively. These assumptions have been previously shown to be reasonable for arterial hemodynamics by several investigators [26]. As suggested in previous studies[13], the Reynolds number ranges from 122 in the end of the diastolic phase to 484 in the peak systolic phase, so the flow can be assumed to be laminar. The flow is considered laminar and the Reynolds number is calculated according to the input velocity and the geometries of the artery. All the calculations are conducted by using commercial software for the time period of 1 s and the flow format of timestep.

#### C. Initial and Boundary Condition

In all of the simulations, to the end of CFD analysis the arterial wall was considered to be rigid, in addition, no slip boundary condition is imposed on the surface of the arterial wall. Mixed velocity-pressure condition is required in order to correctly calculate flow features in CFD analysis. For dynamic simulation, a typical LAD flow waveform introduced by Davies et al. [33] is imposed at the inlet plug velocity profile (Fig. 4), by using the mentioned reference; the specific pressure of 11597 pa is defined as an outlet on the branches. In static simulation, the pulsatile and waveform behavior of the blood flow is ignored and the steady velocity with the amount of 0.17 m/s imposed on the inlet.

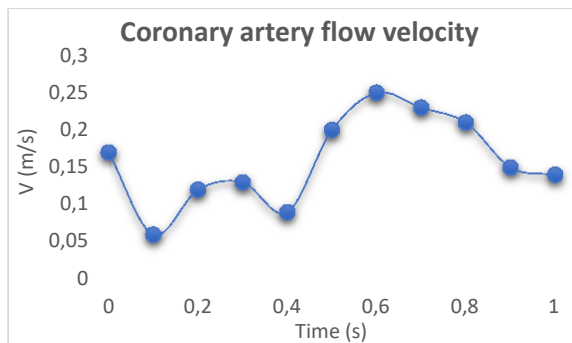


Fig. 4 Coronary artery flow velocity

### III. RESULT

Although the blood flow in the vessels has pulsatile characteristics, sometimes in some studies the uniform flow is considered in order to analyze the hemodynamics. It is generally believed that the WSS is an important hemodynamic variable in the onset of atherosclerotic lesions and this reflect the complex nature of the WSS patterns in the left coronary artery system. According to the presumption of the problem, static and dynamic CFD simulations were performed on bifurcation with angles 30°, 45°, 60°. Both stable and dynamic simulations show the relationship between the maximum value of the speed and bifurcation angulation. Fig. 5 shows the contour of the velocity distribution in different bifurcation angles in static condition. In all of the cases, although the flow has laminar characteristics in the left main coronary artery, by reaching to the bifurcation the flow loses its laminar

characteristics, and the contours of velocity distribution completely changed. In this change of the velocity the shape and the angle of the bifurcation and also the change of the cross-sectional area play an important role. The maximum amount of the speed in static analysis for bifurcation angle  $30^\circ$ ,  $45^\circ$ ,  $60^\circ$  are 0.27 m/s, 0.2689 m/s, 0.265 m/s, respectively. The results show that the maximum value of the speed is decreased by increasing the bifurcation angle. The CFD analysis also showed that the small region of low-velocity blood flow distributed in small angled model gradually increases by increasing the angle. Since the low-velocity

places are posed to flow separation, increasing the angle can contribute to increasing the chance of flow separation.

As it was mentioned in order to simulate the dynamic condition, a typical LAD flow waveform is imposed at the inlet plug. In the dynamic simulation, the value of the input velocity is changed according to time, and as it is shown in Fig. 6 the velocity distribution in bifurcation during the cardiac cycle completely changed. According to this figure, the maximum speed contributed to that time when the inlet velocity reaches its own maximum,  $t=0.65$  s. After this time, the maximum velocity is decreased again.

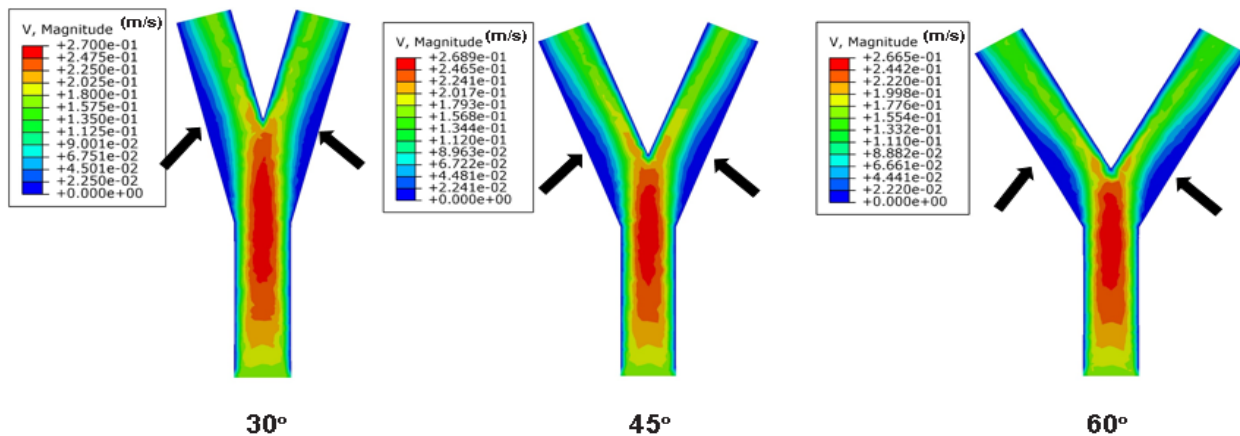


Fig. 5 Distribution of blood flow in static condition

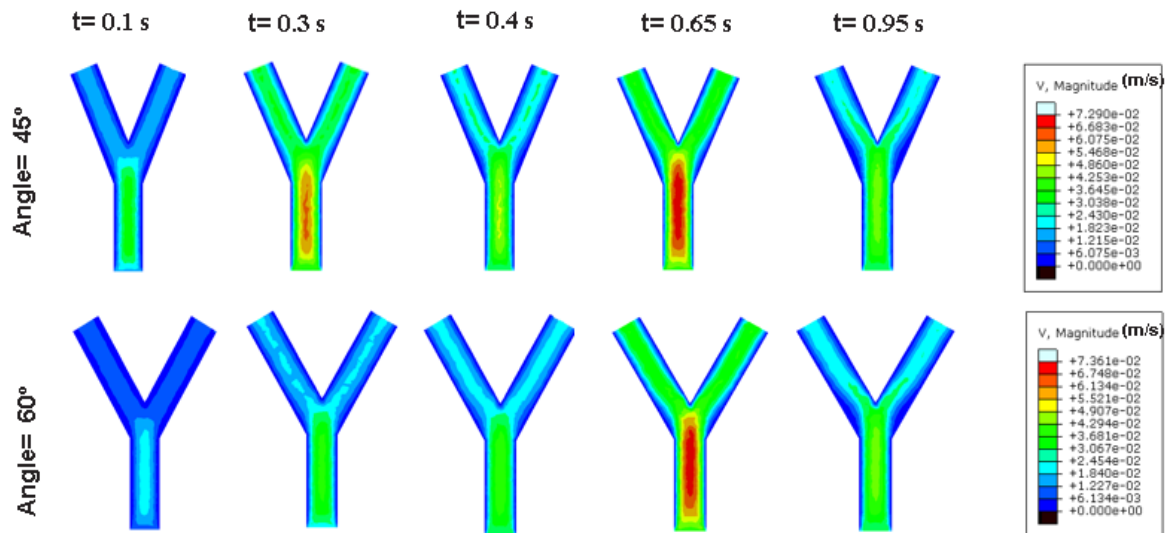


Fig. 6 Velocity distribution during different time



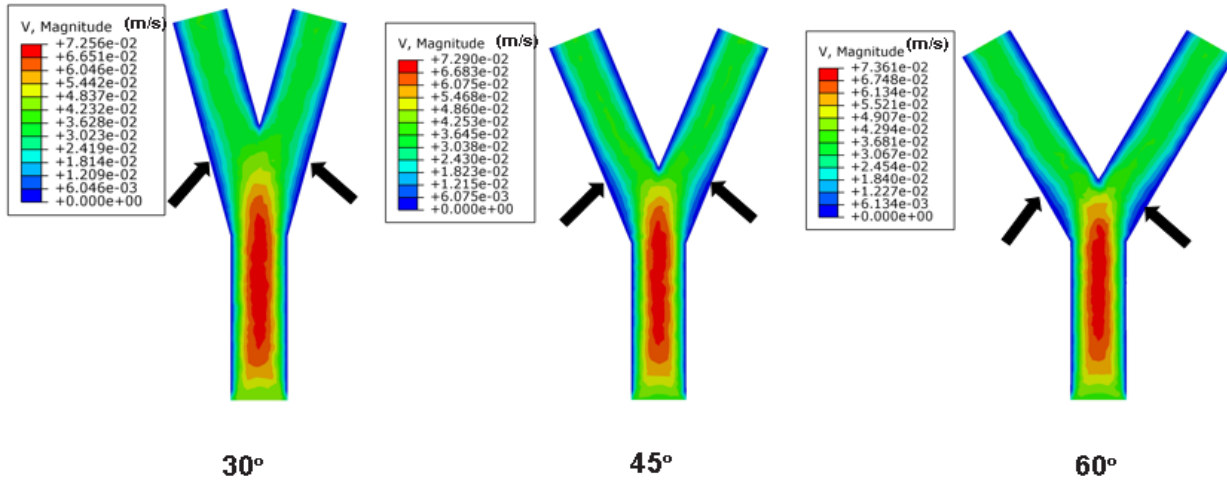


Fig. 7 Velocity blood flow distribution in dynamic condition

Fig. 7 shows the result of the dynamic simulation in bifurcations. There is a discrepancy between the velocity contour when the maximum speed is reached in dynamic condition and the contour of velocity in static condition. While the velocity, in static condition has its maximum in bifurcation section at beginning of the branches, in a dynamic condition the maximum velocity just happened before the bifurcation. The maximum speeds of the bifurcation with angles equal to 30°, 45°, 60° are 0.07256 m/s, 0.07290 m/s, 0.07361 m/s respectively. According to these results, the maximum velocity of the blood flow by increasing the bifurcation angle is increased. In comparison to static analysis, in the dynamic analysis when the maximum speed happens small region of low-velocity blood flow distribution exists, but during the cardiac cycle as shown in Fig. 6, this region completely changed during different steps of the total cycle. In another word, low-velocity near the wall endure the higher variation during dynamic simulation, but the low-velocity region increases with increasing the bifurcation angle and this result agree with results obtained from other works [23].

#### IV. DISCUSSION

Geometry has been recognized as possible risk factor for plaque localization for long time, because of its influence on intra-vascular and near-wall flow patterns [34]. In this study, the influence of changing the angle on velocity blood flow distribution in static and dynamic condition is being investigated. Velocity has a great influence on the WSS, so identifying the correct velocity blood flow distribution is the first step in CFD analysis of the artery's hemodynamic. According to the equation defined in [35], [36], TAWss can be written as:

$$Cf = \frac{2\tau_w}{\rho U^2} \quad (1)$$

$$TAWss = \frac{1}{T} \int_0^T \tau_w dt \quad (2)$$

In (1),  $\rho$  is the density,  $U$  is velocity  $\tau_w$  is the local WSS and it is defined as  $\tau_w = \mu \left( \frac{\partial \bar{U}}{\partial y} \right)$  where  $\mu$  is the blood viscosity,  $\bar{U}$  is velocity near wall perpendicular to surface and  $y$  is distance to the wall surface. According to the proposed equation, it is clear that  $C_f$  is completely related to the velocity. In (2), TAWss is the time average WSS during cardiac systole.  $U$  is defined as the velocity and  $\tau_w$  is the function of the velocity. If we consider  $C_f$  remains constant, then  $\tau_w$  has direct relation with velocity. In the other words, in the condition of presuming skin friction coefficient to be constant, increasing the velocity leads to increasing the final  $\tau_w$ . By increasing the  $\tau_w$ , TAWss is also increased so WSS is increased. If we define (A) according to the bellowed formula:

$$A = \frac{2\tau_w}{\rho U^2} \quad (3)$$

Then, A is clearly has reverse relation with speed. In our study, the region where the maximum velocity happened, is similar to the results of the previous studies; also, the place of the separation of the flow from the wall, agrees with previous studies [37]. The main aim of this study is investigating the relationship between maximum blood flow velocity and angle variation, and in the second step, the efficacy of using dynamic flow instead of static flow for simulating the hemodynamics of blood. Sketches in Fig. 8 show the relationship between the static and dynamic flow with bifurcation angle. Whenever the static flow is imposed in the simulation, by increasing the angle the maximum velocity decreased, but whenever the pulsatile flow imposed in the simulation, the maximum velocity is increased by increasing the angle [38].

By comparing the results contributed to the static condition and results contributed to the dynamic simulation, it is clear that the static condition cannot satisfy the requirement of hemodynamic characteristics of the blood as dynamic condition, and there is the discrepancy between the results obtained from static analysis and the result obtained from the

dynamic analysis.

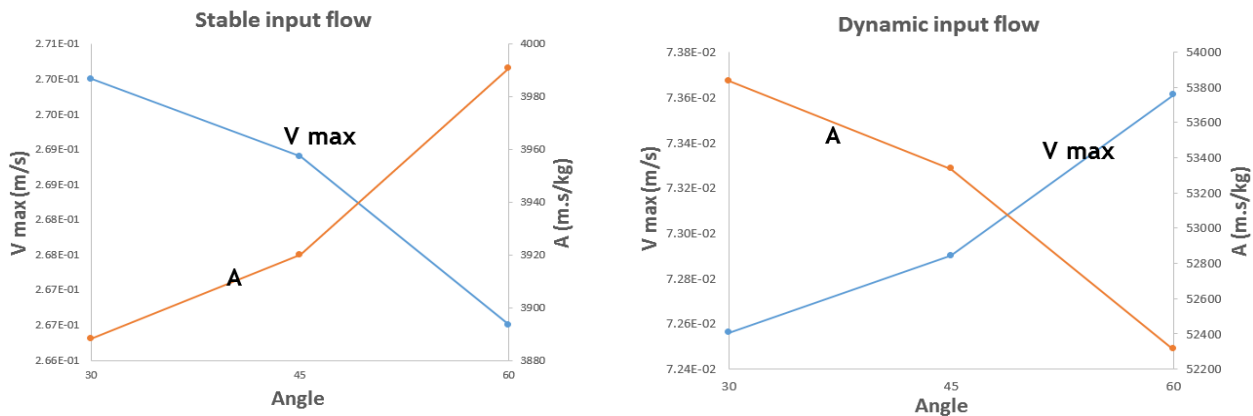


Fig. 8 Relationship between velocity and angle

There is some limitation in our studies. First, we consider the artery's wall as a rigid wall rather than the elastic wall. In our simulations, the coronary wall movement is ignored and the blood considered as a Newtonian, while in some studies suggested considering the blood as non-Newtonian fluid. In this study, the simple model of bifurcation is used and the details of the real artery are ignored. Finally, since the aim of the study is to analyze the difference of velocity distribution in static condition and dynamic simulation, the relationship between WSS and velocity is just introduced by using an equation, for more detailed analysis of WSS and its relationship with velocity, the precise contour of WSS must be plotted.

#### V. CONCLUSION

The geometry of the artery can be an influential factor in CVDs, and investigating the geometry of the arteries can give prediction by introducing the risk potential region in arteries. In this study, the CFD modeling of left coronary artery bifurcation is conducted. Two static and dynamic condition investigated on three different bifurcations with three different angles of 30°, 45°, 60°. The results show that considering the static condition during the simulation leads to the discrepancy between the calculated static simulation and dynamic simulation. In static simulation, we conclude that the results do not match with the other results but the dynamic simulation is considered a realistic simulation and results are similar to other researcher's studies.

Although in both dynamic and static simulations, the region of low-velocity flow distribution near the wall is increased by increasing the bifurcation angle, while the increase of the angle in static analysis leads to decrease the maximum value of velocity, the increase of the angle in dynamical simulations leads to increase the amount of maximum velocity. So it can be concluded that WSS can increase by increasing the bifurcation angle. Since blood flow has the pulsatile characteristics using the uniform velocity during the simulations can lead to the discrepancy between the actual

results and the calculated results.

#### REFERENCES

- [1] G. Lorenzini, and E. J. J. o. B. Casalena, "CFD analysis of pulsatile blood flow in an atherosclerotic human artery with eccentric plaques," vol. 41, no. 9, pp. 1862-1870, 2008.
- [2] P. Y. M. a. H. M., "Technical Brief: Computational Fluid Dynamic (Cfd) Analysis Of Blood Flow Through Human Arteries," *Journal of Computational Simulation and Modeling*, vol. Volume 2, no. Issue 1, pp. 27-29, 2012.
- [3] V. C. Rispoli, J. F. Nielsen, K. S. Nayak *et al.*, "Computational fluid dynamics simulations of blood flow regularized by 3D phase contrast MRI," vol. 14, no. 1, pp. 110, 2015.
- [4] T. G. Papaioannou, and C. J. H. J. C. Stefanadis, "Vascular wall shear stress: basic principles and methods," vol. 46, no. 1, pp. 9-15, 2005.
- [5] C. Chiastra, S. Morlacchi, S. Pereira *et al.*, "Computational fluid dynamics of stented coronary bifurcations studied with a hybrid discretization method," vol. 35, pp. 76-84, 2012.
- [6] A. E. Moran, G. A. Roth, J. Narula *et al.*, "1990-2010 global cardiovascular disease atlas," vol. 9, no. 1, pp. 3-16, 2014.
- [7] W. Quanyu, L. Xiaojie, P. Lingjiao *et al.*, "Simulation Analysis Of Blood Flow In Arteries Of The Human Arm," vol. 29, no. 04, pp. 1750031, 2017.
- [8] F. M. Box, R. J. van der Geest, M. C. Rutten *et al.*, "The influence of flow, vessel diameter, and non-newtonian blood viscosity on the wall shear stress in a carotid bifurcation model for unsteady flow," vol. 40, no. 5, pp. 277-294, 2005.
- [9] M. Malvè, A. Garcia, J. Ohayon *et al.*, "Unsteady blood flow and mass transfer of a human left coronary artery bifurcation: FSI vs. CFD," vol. 39, no. 6, pp. 745-751, 2012.
- [10] J. Ohayon, A. M. Gharib, A. Garcia *et al.*, "Is arterial wall-strain stiffening an additional process responsible for atherosclerosis in coronary bifurcations?: an in vivo study based on dynamic CT and MRI," vol. 301, no. 3, pp. H1097-H1106, 2011.
- [11] S. N., "CFD analysis of blood flow through stenosed arteries," 2015.
- [12] C. M. Scotti, J. Jimenez, S. C. Muluk *et al.*, "Wall stress and flow dynamics in abdominal aortic aneurysms: finite element analysis vs. fluid-structure interaction," vol. 11, no. 3, pp. 301-322, 2008.
- [13] S. Morlacchi, C. Chiastra, D. Gastaldi *et al.*, "Sequential structural and fluid dynamic numerical simulations of a stented bifurcated coronary artery," vol. 133, no. 12, pp. 121010, 2011.
- [14] U. Lee, B. Seo, I. J. J. o. m. s. Jang *et al.*, "Spectral element modeling and analysis of the blood flow through a human blood vessel," vol. 22, no. 8, pp. 1612-1619, 2008.
- [15] G. Giannoglou, J. Soulis, T. Farmakis *et al.*, "Haemodynamic factors and the important role of local low static pressure in coronary wall thickening," vol. 86, no. 1, pp. 27-40, 2002.
- [16] M. Mehrabi, and S. J. M. P. i. E. Setayeshi, "Computational fluid dynamics analysis of pulsatile blood flow behavior in modelled stenosed

- vessels with different severities," vol. 2012, 2012.
- [17] S. H. Lee, S. Kang, N. Hur *et al.*, "A fluid-structure interaction analysis on hemodynamics in carotid artery based on patient-specific clinical data," vol. 26, no. 12, pp. 3821-3831, 2012.
  - [18] R. Torii, M. Oshima, T. Kobayashi *et al.*, "Role of 0D peripheral vasculature model in fluid-structure interaction modeling of aneurysms," vol. 46, no. 1, pp. 43-52, 2010.
  - [19] D. Zeng, E. Boutsianis, M. Ammann *et al.*, "A study on the compliance of a right coronary artery and its impact on wall shear stress," vol. 130, no. 4, pp. 041014, 2008.
  - [20] S. Tada, and J. J. A. o. b. e. Tarbell, "A computational study of flow in a compliant carotid bifurcation-stress phase angle correlation with shear stress," vol. 33, no. 9, pp. 1202-1212, 2005.
  - [21] S. H. Lee, H. G. Choi, J. Y. J. J. o. M. S. Yool *et al.*, "Finite element simulation of blood flow in a flexible carotid artery bifurcation," vol. 26, no. 5, pp. 1355-1361, 2012.
  - [22] X. Han, R. Bibb, R. J. J. o. V. L. Harris *et al.*, "Design of bifurcation junctions in artificial vascular vessels additively manufactured for skin tissue engineering," vol. 28, pp. 238-249, 2015.
  - [23] Z. Sun, and Y. J. E. j. o. r. Cao, "Multislice CT angiography assessment of left coronary artery: correlation between bifurcation angle and dimensions and development of coronary artery disease," vol. 79, no. 2, pp. e90-e95, 2011.
  - [24] S. Beier, J. Ormiston, M. Webster *et al.*, "Impact of bifurcation angle and other anatomical characteristics on blood flow-A computational study of non-stented and stented coronary arteries," vol. 49, no. 9, pp. 1570-1582, 2016.
  - [25] F. Migliavacca, L. Petrini, V. Montanari *et al.*, "A predictive study of the mechanical behaviour of coronary stents by computer modelling," vol. 27, no. 1, pp. 13-18, 2005.
  - [26] S. Smith, S. Austin, G. D. Wesson *et al.*, "Calculation of wall shear stress in left coronary artery bifurcation for pulsatile flow using two-dimensional computational fluid dynamics," pp. 871-874.
  - [27] M. Prosi, K. Perktold, Z. Ding *et al.*, "Influence of curvature dynamics on pulsatile coronary artery flow in a realistic bifurcation model," vol. 37, no. 11, pp. 1767-1775, 2004.
  - [28] X. Han, R. Bibb, and R. J. P. C. Harris, "Artificial Vascular Bifurcations-Design and Modelling," vol. 49, pp. 14-18, 2016.
  - [29] G. A. Rodriguez-Granillo, M. A. Rosales, E. Degrossi *et al.*, "Multislice CT coronary angiography for the detection of burden, morphology and distribution of atherosclerotic plaques in the left main bifurcation," vol. 23, no. 3, pp. 389-392, 2007.
  - [30] T. Chaichana, Z. Sun, and J. J. J. o. b. Jewkes, "Computation of hemodynamics in the left coronary artery with variable angulations," vol. 44, no. 10, pp. 1869-1878, 2011.
  - [31] C. Chiastra, D. Gallo, P. Tasso *et al.*, "Healthy and diseased coronary bifurcation geometries influence near-wall and intravascular flow: A computational exploration of the hemodynamic risk," vol. 58, pp. 79-88, 2017.
  - [32] S. Bahrami, and F. Firouzi, "The effect of wall shear stress and oscillatory shear index on probability of atherosclerosis plaque formation in normal left coronary artery tree," 2016.
  - [33] J. E. Davies, Z. I. Whinnett, D. P. Francis *et al.*, "Evidence of a dominant backward-propagating "suction" wave responsible for diastolic coronary filling in humans, attenuated in left ventricular hypertrophy," vol. 113, no. 14, pp. 1768-1778, 2006.
  - [34] K. K. Wong, P. Thavornpattanaong, S. C. Cheung *et al.*, "Effect of calcification on the mechanical stability of plaque based on a three-dimensional carotid bifurcation model," vol. 12, no. 1, pp. 7, 2012.
  - [35] M. Golozar, M. Sayed Razavi, and E. J. S. I. Shirani, "Theoretical and computational investigation of optimal wall shear stress in bifurcations: a generalization of Murray's law," vol. 24, no. 5, pp. 2387-2395, 2017.
  - [36] A. Arzani, and S. C. J. J. o. b. e. Shadden, "Characterizations and correlations of wall shear stress in aneurysmal flow," vol. 138, no. 1, pp. 014503, 2016.
  - [37] Y.-c. Fung, *Biomechanics: mechanical properties of living tissues*: Springer Science & Business Media, 2013.
  - [38] R. Torii, N. B. Wood, N. Hadjiloizou *et al.*, "Fluid-structure interaction analysis of a patient-specific right coronary artery with physiological velocity and pressure waveforms," vol. 25, no. 5, pp. 565-580, 2009.